Report

Current Biology

Olfaction Modulates Reproductive Plasticity through Neuroendocrine Signaling in *Caenorhabditis elegans*

Graphical Abstract

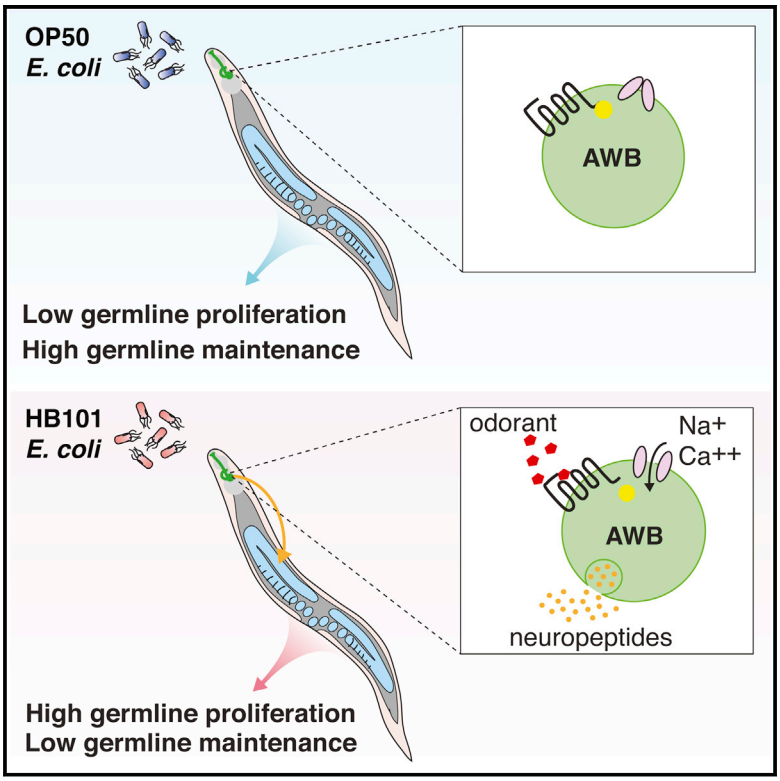

Highlights

- Animals adjust reproductive strategy in response to environmental variations
- AWB olfactory neurons regulate reproductive plasticity
- Neuropeptide signaling mediates the olfactory regulation of reproductive aging

Authors

Jessica N. Sowa, Ayse Sena Mutlu, Fan Xia, Meng C. Wang

Correspondence

wmeng@bcm.edu

In Brief

Sowa et al. show that AWB olfactory neurons perceive odorant signals to adjust reproductive timing and senescence via neuropeptide signaling, revealing a neuroendocrine link between olfactory sensation and reproductive plasticity and the power of smell to regulate reproductive aging.

Sowa et al., 2015, Current Biology *25*, 2284–2289
August 31, 2015
http://dx.doi.org/10.1016/j.cub.2015.07.023

CellPress

CellPress

Current Biology
Report

Olfaction Modulates Reproductive Plasticity through Neuroendocrine Signaling in *Caenorhabditis elegans*

Jessica N. Sowa,[1,2] Ayse Sena Mutlu,[3] Fan Xia,[2] and Meng C. Wang[1,2,3,*]
[1]Huffington Center on Aging, Baylor College of Medicine, Houston, TX 77030, USA
[2]Department of Molecular and Human Genetics, Baylor College of Medicine, Houston, TX 77030, USA
[3]Program in Developmental Biology, Baylor College of Medicine, Houston, TX 77030, USA
*Correspondence: wmeng@bcm.edu
http://dx.doi.org/10.1016/j.cub.2015.07.023

SUMMARY

Reproductive plasticity describes the ability of organisms to adjust parameters such as volume, rate, or timing of progeny production in order to maximize successful reproduction under different environmental conditions. Reproductive plasticity in response to environmental variation has been observed in a wide range of animals [1–4]; however, the mechanisms involved in translating environmental cues into reproductive outcomes remain unknown. Here, we show that olfaction modulates reproductive timing and senescence through neuroendocrine signaling in *Caenorhabditis elegans*. On their preferred diet, worms demonstrate an increased rate of reproduction and an early onset of reproductive aging. Perception of the preferred diet's odor by AWB olfactory neurons elicits these adjustments by increasing germline proliferation, and optogenetic stimulation of AWB neurons is sufficient to accelerate reproductive timing in the absence of dietary inputs. Furthermore, AWB neurons act through neuropeptide signaling to regulate reproductive rate and senescence. These findings reveal a neuroendocrine nexus linking olfactory sensation and reproduction in response to environmental variation and indicate the significance of olfaction in the regulation of reproductive decline during aging.

RESULTS AND DISCUSSION

As soil-dwelling nematodes, *C. elegans* experience their diet of bacteria as a source of both sensory and nutritional inputs from the environment. To test whether *C. elegans* responds to environmental variations with different reproductive strategies, we examined the reproductive lifespan of wild-type *C. elegans* feeding on different bacterial diets, including *Comamonas sp.*, *Bacillus megaterium*, and a number of *Escherichia coli* strains (OP50, HB101, HT115, and MG1655) and found distinct differences among them (Figure S1A).

In particular, the reproductive lifespan of wild-type *C. elegans* feeding on HB101 *E. coli* was ~65% shorter than that of worms feeding on OP50 *E. coli* (Figure 1A; Table S1), although these two *E. coli* strains are closely related. *C. elegans* feeding on OP50 and HB101 had comparable brood size (Figure 1B), development (Figure S1B), and lifespan [5, 6]. Both food intake rate (Figure S1C) and physical activity (Figure S1D) were slightly changed in worms raised on HB101. HB101 exposure at different developmental stages decreased reproductive lifespan to a similar extent (Figure 1C; Table S2), even at day 1 adult stage when the germline has fully developed and differentiated [7]. On the other hand, exposure to OP50 at different developmental stages induced reproductive lifespan extension, but a prolonged period of exposure was necessary to negate the effect of prior exposure to HB101 (Figure S1E; Table S2). Together, these results suggest that the difference in reproductive lifespan is not simply a result of altered germline development or maturation.

Wild-type *C. elegans* feeding on HB101 had an accelerated rate of reproduction for the first 2 days of adulthood, followed by early reproductive cessation (Figure 1D). Consistently, these animals showed 37% more EdU-positive S phase nuclei in the germline compared to their counterparts on OP50 after 1-hr pulse labeling (Figure 1E), indicating that HB101 exposure increases the rate of germline proliferation. Furthermore, wild-type *C. elegans* raised on OP50 and switched to HB101 at L4 stage or day 1 of adulthood also showed increased EdU-positive nuclei compared to OP50-only controls (Figure S1F), suggesting that the rate of germline proliferation is rapidly modulated upon HB101 exposure. *C. elegans* hermaphrodites cease reproduction upon self-sperm exhaustion and can resume reproduction when supplied with young sperm; however, fertility during late mating declines with hermaphrodite age and the concomitant failure of oocyte maintenance [8–10]. We mated post-self-reproductive wild-type hermaphrodites at different ages with young males and found that HB101 exposure significantly decreased success of late conception with fresh sperm (Figure 1F), suggesting an earlier onset of reproductive senescence. Thus, in responding to different bacterial environmental inputs, *C. elegans* adopt different reproductive strategies by adjusting both the rate of germline proliferation and the onset of reproductive aging. Interestingly, computational simulation suggested that the HB101-associated reproductive strategy is advantageous in an unsaturated environment where population size is much smaller than environmental capacity, whereas the OP50 one is more

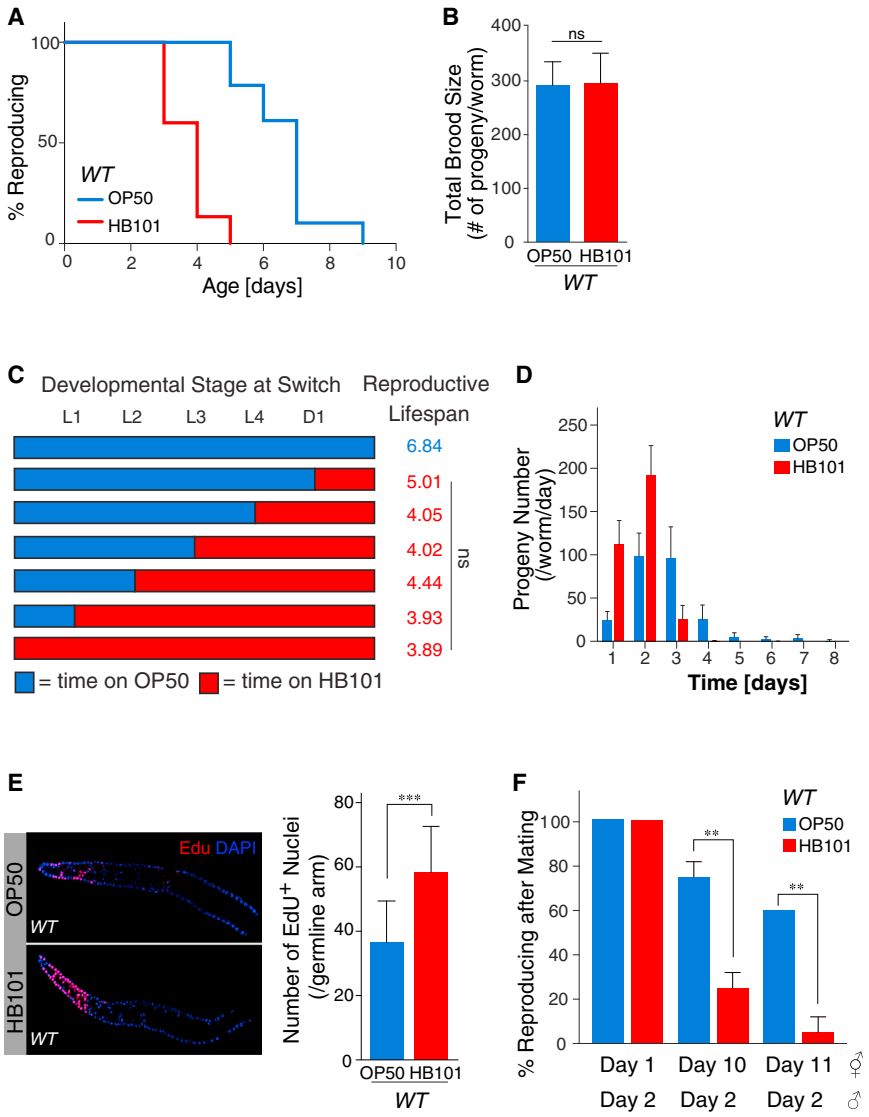

Figure 1. Reproductive Strategy Is Adjusted under Dietary Variations

(A) Wild-type (WT) worms feeding on *E. coli* HB101 show a significantly shorter reproductive lifespan compared to those on *E. coli* OP50 ($p < 0.001$; log rank test).

(B) Total progeny numbers of WT worms feeding on OP50 and HB101 are not significantly different ($p > 0.05$; Student's t test; n = 20). Data are represented as mean ± SD.

(C) WT worms feeding on OP50 were switched to HB101 at the L1, L2, L3, L4, or day 1 adult stage, and their reproductive lifespans are not significantly different from that of WT worms feeding entirely on HB101 ($p > 0.05$; log rank test).

(D) WT worms feeding on HB101 have an accelerated rate of progeny production in early adulthood and an early onset of reproductive cessation. Data are represented as mean ± SD.

(E) Germline proliferation assessment by EdU incorporation shows that WT worms feeding on HB101 have a significantly higher number of EdU-positive nuclei per germline arm compared to those feeding on OP50 (***$p < 0.001$; Student's t test). Data are represented as mean ± SD.

(F) WT hermaphrodites were crossed with 2-day-old young males at indicated ages. Compared to OP50-feeding worms, the success rate of late conception is decreased in HB101-feeding worms by 3-fold at day 10 age and 12-fold at day 11 age (**$p < 0.01$; Fisher's exact test; n = 20). Data are represented as mean ± SD.

See also Figure S1.

advantageous when the environment becomes saturated (Figure S1G).

Next, to investigate the origin and nature of the bacterial inputs, we measured the reproductive lifespans of *C. elegans* feeding on mixtures of HB101 and OP50. To our surprise, worms raised on bacterial mixtures containing diluted HB101 (1:1, 1:10, and 1:100) showed reproductive lifespans indistinguishable from those of worms feeding on HB101 alone (Figure 2A; Table S2). Feeding HB101 and OP50 strains expressing mCherry and GFP, respectively, confirmed that animals consumed both bacterial types in the mixture. The very low detection threshold for the reproductive response to HB101 and the relatively short time needed to initiate this response (Figure 1C) are consistent with the ability of *C. elegans* to detect volatile chemicals at low concentrations [11].

To test whether the regulatory cues associated with HB101 were volatile signals, we incubated worms in chambers designed to allow them to feed on one bacterial strain while smelling a second strain (Figure 2B). We found that exposure to the odor of HB101 alone significantly reduced the reproductive lifespan of wild-type worms feeding on OP50 (Figure 2C; Table S1). These findings indicate that volatile odorants derived from HB101 bacteria act as the signal to affect reproductive timing.

C. elegans olfaction is mediated by G-protein-coupled receptors (GPCRs) on chemosensory neurons, which utilize a few different Gα subunits [11, 12]. We found that mutants lacking *odr-3*, a Gα subunit expressed in AWA, AWB, AWC, and ADF olfactory neurons [13], displayed an OP50-like reproductive lifespan on both OP50 and HB101 (Figure 3A; Table S1). We further analyzed mutants specifically defective in each of the neuron classes affected by the *odr-3*(*n2046*) mutation and found that the *lim-4*(*ky403*) mutant, which lacks a transcription factor necessary for AWB neuronal fate specification and thus functional AWB neurons [14], showed an OP50-like reproductive lifespan on both OP50 and HB101 (Figure 3B; Table S1). The *lim-4* mutant also failed to shorten reproductive lifespan when exposed to HB101 odors (Figure S2; Table S1). Mutations affecting AWA, AWC, or ADF neurons, however, did not alleviate reproductive lifespan differences on HB101 versus OP50 (Figure S3; Table S1). Restoring *odr-3* expression exclusively in AWB neurons was sufficient to rescue the reproductive lifespan difference in the *odr-3* mutant (Figure 3C; Table S1). Together,

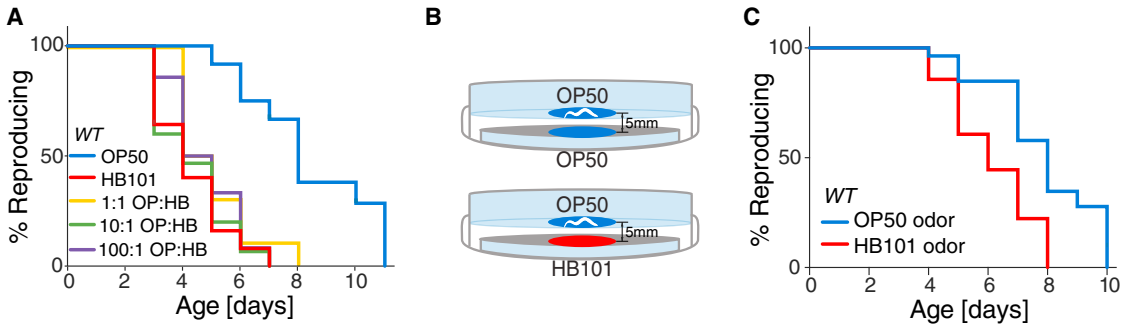

Figure 2. Volatile Sensory Cues Elicit Reproductive Timing Adjustment

(A) Reproductive lifespan of WT worms feeding on OP50 and HB101 mixed in varying ratios (1:1, 10:1, and 100:1 OP50:HB101) are indistinguishable from those on HB101 alone ($p > 0.05$; log rank test).

(B) Design of 3D-printed odor exposure chambers. Adult worms are fed on OP50 while exposed to the odorants of either HB101 or OP50. The distance between two agar surfaces is 5 mm.

(C) Exposure to HB101 odorants significantly reduces the reproductive lifespan of WT worms feeding on OP50 ($p < 0.01$; log rank test).

See also Figure S2.

these results suggest that AWB neurons are specifically required in perceiving HB101-derived sensory inputs to adjust reproductive timing. Furthermore, *odr-3* and *lim-4* mutants grown on HB101 showed low rates of germline proliferation similar to that of wild-type worms on OP50 (Figures 1E and 3D), indicating that AWB neurons modulate reproductive timing by affecting germline proliferation.

We next photoactivated AWB neurons, using a transgenic line (*AWB*::*ChR2 Tg*) expressing the blue-light-activated cation channel channelrhodopsin-2 (ChR2) [15] under the control of the AWB-specific *str-1* promoter [16]. Unstimulated *AWB*::*ChR2 Tg* animals showed a 43% longer reproductive lifespan on OP50 than on HB101 (Figure 3E; Table S1); however, this extension was completely abolished in *AWB*::*ChR2 Tg* animals upon blue light activation (Figure 3E; Table S1). Blue light exposure did not affect reproductive lifespan difference of wild-type animals on HB101 versus OP50 (Figure 3E; Table S1). Thus, AWB neuronal activation is sufficient to recapitulate the effect of HB101-derived sensory signals on reproductive timing.

C. elegans neurotransmission is mediated by both neurotransmitters and neuropeptides, which are released synaptically from small clear vesicles (SCVs) and non-synaptically from dense core vesicles (DCVs), respectively [17, 18]. We blocked SCV release specifically in AWB neurons by expressing tetanus toxin light chain [19] using the *str-1* promoter and found that inhibition of neurotransmitter signaling did not alleviate the reproductive lifespan difference on HB101 versus OP50 (Figure 4A; Table S1). Next, we inhibited neuropeptide release from AWB neurons by expressing dsRNA against *C. elegans* CAPS homolog UNC-31 (*AWB*::*unc-31*^{KD}), which is necessary for DCV, but not SCV, release [20]. *AWB*::*unc-31*^{KD} transgenic strains did not show differences in reproductive lifespan when grown on HB101 versus OP50 (Figure 4B; Table S1). Furthermore, *AWB*::*unc-31*^{KD} transgenic worms grown on OP50 and HB101 both showed increased success of late-life fertilization (Figure 4C). Thus, neuropeptide signaling of AWB neurons mediates the olfactory impacts on both reproductive rate and reproductive senescence.

Previous reports indicated that chemosensory neurons mediate *C. elegans* choice to different bacteria [21–23]. Given the strong preference of wild-type worms for HB101 (Figure 4D) [24], we tested whether AWB neuropeptide signaling mediates this response. We found that the preference for HB101 was completely abolished in the *lim-4*(*ky403*) mutant and in the mutants *egl-3*(*gk238*), *egl-21*(*n476*), and *sbt-1*(*ok901*) that are defective in neuropeptide synthesis and processing [25–27] (Figure 4D). These results suggest that AWB olfactory neurons perceive environmental cues and consequently modulate both the organisms' attraction behavior and reproductive strategies via neuropeptide transmission.

Together, our results reveal that olfactory neuroendocrine signaling regulates reproductive strategies in response to environmental cues. Based on computational simulation, HB101- and OP50-related reproductive strategies correlate with survival advantages under unsaturated and saturated environments, respectively. Interestingly, experimental results show that animals prefer the HB101 environment, suggesting that the HB101-associated volatile signal may act as an indicator of a favorable environment with high capacity. The olfactory regulatory mechanism would give organisms flexibility for rapidly responding to environmental fluctuations and adjusting reproductive strategies to ensure the perpetuation of the species.

Our studies also suggest a reverse correlation between early- and late-life fertility under different environments. Although *C. elegans* continues to produce oocytes throughout adult life, the quality of oocytes decline with age [8], resulting in late-life fertility defects. Further study is needed to determine whether the late-life fertility defect associated with HB101 exposure is a direct consequence of the increased rate of germline proliferation in earlier life or whether the two effects could potentially be uncoupled. Notably, a similar trade-off has also been demonstrated in experimental evolution studies in both *C. elegans* [28] and *Drosophila* [29]. Therefore, early- and late-life fertility may be inextricably linked and their trade-off may be under the control of the olfactory nervous system. Olfactory regulation of early-life fertility via hormonal signaling is well known in mammals [30]; our findings therefore raise the possibility that olfactory neuroendocrine signaling could be also contributing to the regulation of reproductive aging in higher organisms.

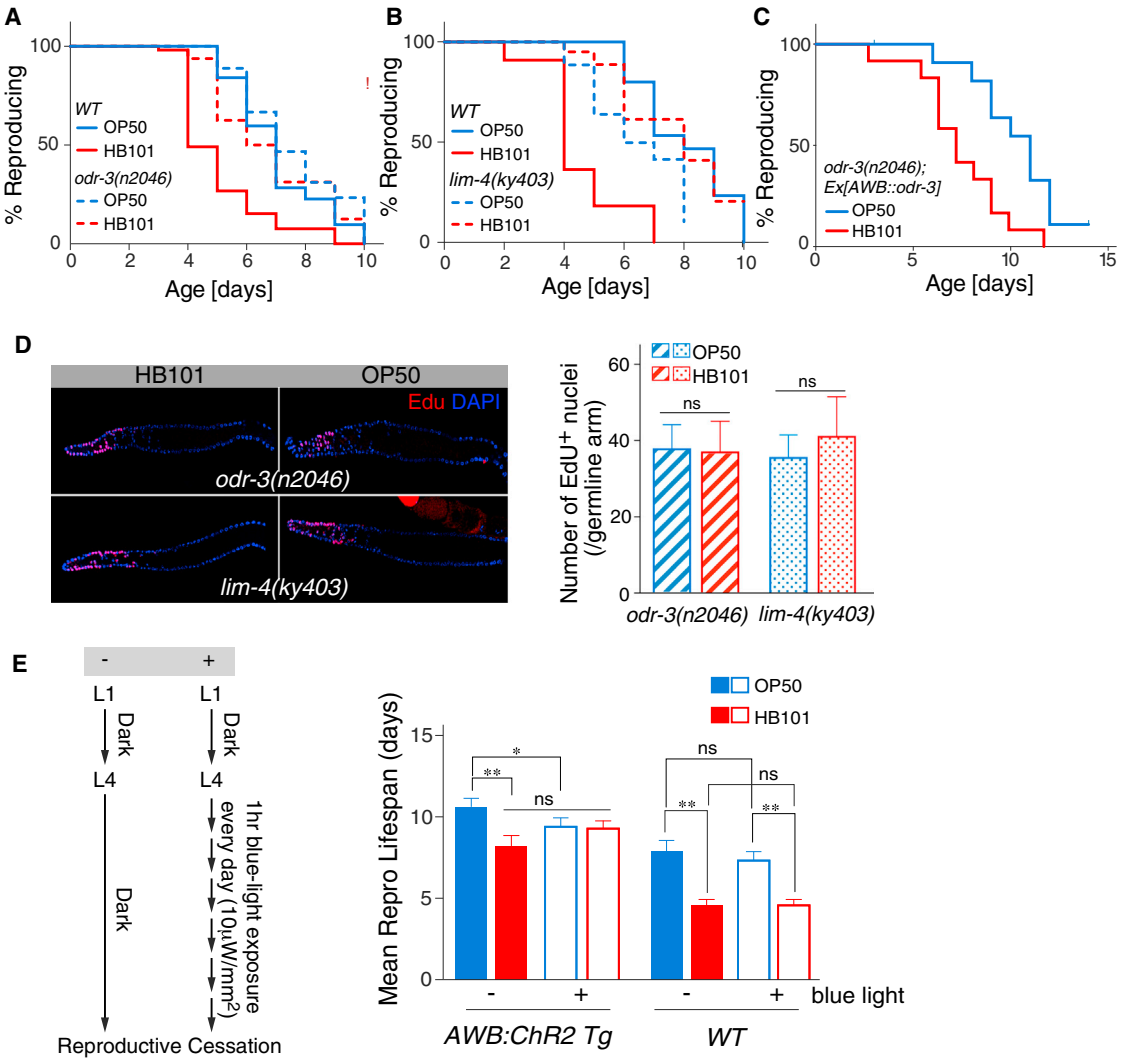

Figure 3. AWB Olfactory Neurons Regulate Reproductive Timing

(A) *odr-3*(*n2046*) olfaction-defective mutants feeding on OP50 and HB101 both show reproductive lifespans similar to that of WT worms feeding on OP50 ($p > 0.05$; log rank test; composite of two trials).

(B) *lim-4*(*ky403*) mutants that lack functional AWB neurons do not show a difference in reproductive lifespan on OP50 versus HB101, with both similar to WT reproductive lifespan on OP50 ($p > 0.05$; log rank test; composite of two trials).

(C) AWB-specific rescue of *odr-3* expression in the *odr-3*(*n2046*) mutants restores difference in reproductive lifespan ($p < 0.001$; log rank test).

(D) Neither the *odr-3*(*n2046*) nor *lim-4*(*ky403*) show differences in numbers of germline EdU+ nuclei between OP50 and HB101 feeding conditions ($p > 0.05$; Student's t test). Data are represented as mean ± SD.

(E) *AWB*::*ChR2* transgenic and WT worms with and without blue light stimulation (as shown in diagram) were compared for reproductive lifespan. Unstimulated *AWB*::*ChR2 Tg* worms show reproductive lifespan differences on OP50 versus HB101 (**$p < 0.01$; log rank test). Blue light stimulation significantly reduces the reproductive lifespan of *AWB*::*ChR2 Tg* worms feeding on OP50 (*$p < 0.05$; log rank test) but does not affect the reproductive lifespan of *AWB*::*ChR2 Tg* worms feeding on HB101 or the reproductive lifespan of WT worms on either OP50 or HB101 ($p > 0.05$; log rank test). Data are represented as mean ± SEM.

See also Figure S3.

Interestingly, genetic interaction analysis showed that this olfactory regulation acts independently of the FOXO/insulin/IGF-1, TGF-β Sma/Mab, or caloric restriction pathways (Figures S3D–S3G), which are thus far the only characterized regulators of *C. elegans* reproductive aging [8, 9]. Thus, our findings suggest an ancient link between the olfactory and reproductive systems and reveal a distinct regulatory mechanism of reproductive aging via neuroendocrine signaling. Further studies will be needed to elucidate the genes and pathways implicated in this regulation, which will provide an entry point for investigating the underlying mechanisms by which the olfactory nervous system modulates the processes of reproductive senescence in higher organisms.

SUPPLEMENTAL INFORMATION

Supplemental Information includes Supplemental Experimental Procedures, three figures, and two tables and can be found with this article online at http://dx.doi.org/10.1016/j.cub.2015.07.023.

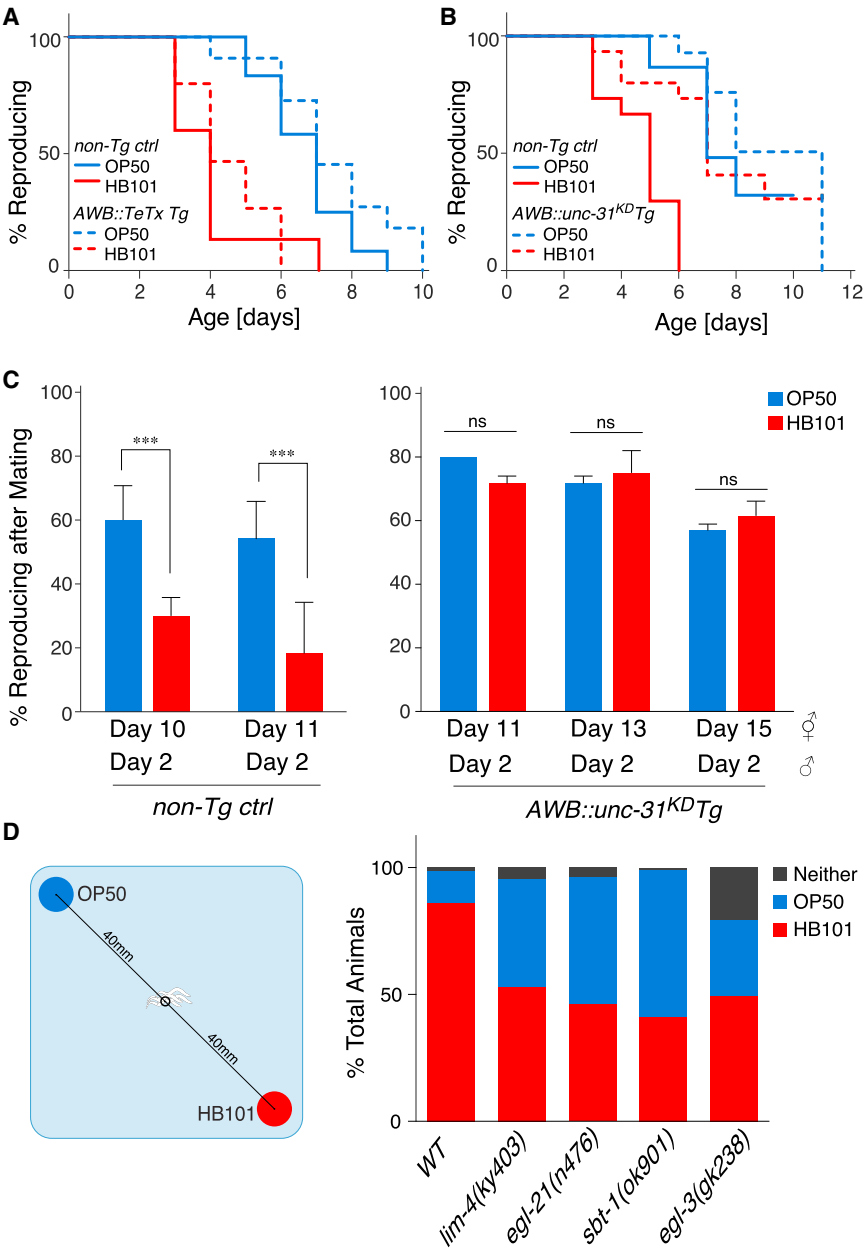

Figure 4. Neuropeptide Signaling Mediates Reproductive and Behavioral Responses

(A) *AWB*::*TeTx* transgenic strains and nontransgenic sibling controls show the same level of differences in reproductive lifespan on OP50 versus HB101 ($p < 0.01$; log rank test).

(B) *AWB*::*unc-31*^{KD} transgenic strains feeding on HB101 and OP50 do not show a significant difference in reproductive lifespan ($p > 0.05$; log rank test), whereas nontransgenic sibling controls show a significant difference ($p < 0.001$; log rank test).

(C) Nontransgenic control or *AWB*::*unc-31*^{KD} transgenic worms crossed with 2-day-old young WT males at indicated ages. Ten-day-old controls show 60% success rate of conception when raised on OP50, compared to 30% on HB101 (***$p < 0.001$; Fisher's exact test; n = 65). Data are represented as mean ± SD. Eleven-day-old controls show 54% success rate of conception when raised on OP50, compared to 18% on HB101 (***$p < 0.001$; Fisher's exact test; n = 50). *AWB*::*unc-31*^{KD} transgenic worms show 76%, 73%, and 64% success rate of conception when raised on either HB101 or OP50 at day 11, day 13, and day 15, respectively ($p > 0.05$; Fisher's exact test; n = 25). Data are represented as mean ± SD.

(D) In the food choice assay, WT worms show 74% (±6%) preference for HB101. This preference is absent in the *lim-4*(*ky403*) mutant and in the neuropeptide-processing mutants *egl-3*(*gk238*), *egl-21*(*n476*), and *sbt-1*(*ok901*). Representative experiment is an average of three technical replicates.

AUTHOR CONTRIBUTIONS

J.N.S., A.S.M., and M.C.W. conceived the study. J.N.S. and A.S.M. performed experiments and analysis. F.X. designed and tested computational simulations. J.N.S., A.S.M., F.X., and M.C.W. wrote the manuscript.

ACKNOWLEDGMENTS

We thank S. Xu, C. Herman, and J. Mello for providing plasmids; M. Mutlu for designing and making a blue LED chamber for optogenetic stimulation experiments; A. Dervisefendic for experimental support; and M. Matzuk and C. Herman for critical reading of this manuscript. This work is supported by NIH grants RO1AG045183 (to M.C.W.), T32GM8307-20 and 5T32AG00183-23 (to J.N.S.), Ellison Medical Foundation New Scholar Award (to M.C.W.), and Burroughs Wellcome Foundation Houston Laboratory and Population Sciences Training Program in Gene-Environment Interaction (to J.N.S.). A.S.M. is a Howard Hughes Medical Institute International Student Research fellow.

Received: June 2, 2015
Revised: July 7, 2015
Accepted: July 9, 2015
Published: August 13, 2015

REFERENCES

1. Gharrett, A.J., Joyce, J., and Smoker, W.W. (2013). Fine-scale temporal adaptation within a salmonid population: mechanism and consequences. Mol. Ecol. *22*, 4457–4469.
2. Lutterschmidt, D.I. (2012). Chronobiology of reproduction in garter snakes: neuroendocrine mechanisms and geographic variation. Gen. Comp. Endocrinol. *176*, 448–455.

3. Reilly, S.J., Oum, R., and Heideman, P.D. (2006). Phenotypic plasticity of reproductive traits in response to food availability and photoperiod in white-footed mice (Peromyscus leucopus). Oecologia *150*, 373–382.
4. Sergio, F., Blas, J., López, L., Tanferna, A., Díaz-Delgado, R., Donázar, J.A., and Hiraldo, F. (2011). Coping with uncertainty: breeding adjustments to an unpredictable environment in an opportunistic raptor. Oecologia *166*, 79–90.
5. Brooks, K.K., Liang, B., and Watts, J.L. (2009). The influence of bacterial diet on fat storage in C. elegans. PLoS ONE *4*, e7545.
6. MacNeil, L.T., Watson, E., Arda, H.E., Zhu, L.J., and Walhout, A.J. (2013). Diet-induced developmental acceleration independent of TOR and insulin in C. elegans. Cell *153*, 240–252.
7. Hubbard, E.J., and Greenstein, D. (2005). Introduction to the germ line. WormBook, 1–4.
8. Luo, S., Kleemann, G.A., Ashraf, J.M., Shaw, W.M., and Murphy, C.T. (2010). TGF-β and insulin signaling regulate reproductive aging via oocyte and germline quality maintenance. Cell *143*, 299–312.
9. Hughes, S.E., Evason, K., Xiong, C., and Kornfeld, K. (2007). Genetic and pharmacological factors that influence reproductive aging in nematodes. PLoS Genet. *3*, e25.
10. Mendenhall, A.R., Wu, D., Park, S.K., Cypser, J.R., Tedesco, P.M., Link, C.D., Phillips, P.C., and Johnson, T.E. (2011). Genetic dissection of late-life fertility in Caenorhabditis elegans. J. Gerontol. A Biol. Sci. Med. Sci. *66*, 842–854.
11. Bargmann, C.I. (2006). Chemosensation in C. elegans. WormBook, 1–29.
12. Lans, H., Rademakers, S., and Jansen, G. (2004). A network of stimulatory and inhibitory Galpha-subunits regulates olfaction in Caenorhabditis elegans. Genetics *167*, 1677–1687.
13. Roayaie, K., Crump, J.G., Sagasti, A., and Bargmann, C.I. (1998). The G alpha protein ODR-3 mediates olfactory and nociceptive function and controls cilium morphogenesis in C. elegans olfactory neurons. Neuron *20*, 55–67.
14. Sagasti, A., Hobert, O., Troemel, E.R., Ruvkun, G., and Bargmann, C.I. (1999). Alternative olfactory neuron fates are specified by the LIM homeobox gene lim-4. Genes Dev. *13*, 1794–1806.
15. Husson, S.J., Gottschalk, A., and Leifer, A.M. (2013). Optogenetic manipulation of neural activity in C. elegans: from synapse to circuits and behaviour. Biol. Cell *105*, 235–250.
16. Troemel, E.R., Kimmel, B.E., and Bargmann, C.I. (1997). Reprogramming chemotaxis responses: sensory neurons define olfactory preferences in C. elegans. Cell *91*, 161–169.
17. Chase, D.L., and Koelle, M.R. (2007). Biogenic amine neurotransmitters in C. elegans. WormBook, 1–15.
18. Li, C., and Kim, K. (2008). Neuropeptides (WormBook), pp. 1–36.
19. Sweeney, S.T., Broadie, K., Keane, J., Niemann, H., and O'Kane, C.J. (1995). Targeted expression of tetanus toxin light chain in Drosophila specifically eliminates synaptic transmission and causes behavioral defects. Neuron *14*, 341–351.
20. Speese, S., Petrie, M., Schuske, K., Ailion, M., Ann, K., Iwasaki, K., Jorgensen, E.M., and Martin, T.F. (2007). UNC-31 (CAPS) is required for dense-core vesicle but not synaptic vesicle exocytosis in Caenorhabditis elegans. J. Neurosci. *27*, 6150–6162.
21. Harris, G., Shen, Y., Ha, H., Donato, A., Wallis, S., Zhang, X., and Zhang, Y. (2014). Dissecting the signaling mechanisms underlying recognition and preference of food odors. J. Neurosci. *34*, 9389–9403.
22. Ha, H.I., Hendricks, M., Shen, Y., Gabel, C.V., Fang-Yen, C., Qin, Y., Colón-Ramos, D., Shen, K., Samuel, A.D., and Zhang, Y. (2010). Functional organization of a neural network for aversive olfactory learning in Caenorhabditis elegans. Neuron *68*, 1173–1186.
23. Meisel, J.D., Panda, O., Mahanti, P., Schroeder, F.C., and Kim, D.H. (2014). Chemosensation of bacterial secondary metabolites modulates neuroendocrine signaling and behavior of C. elegans. Cell *159*, 267–280.
24. Shtonda, B.B., and Avery, L. (2006). Dietary choice behavior in Caenorhabditis elegans. J. Exp. Biol. *209*, 89–102.
25. Husson, S.J., Clynen, E., Baggerman, G., Janssen, T., and Schoofs, L. (2006). Defective processing of neuropeptide precursors in Caenorhabditis elegans lacking proprotein convertase 2 (KPC-2/EGL-3): mutant analysis by mass spectrometry. J. Neurochem. *98*, 1999–2012.
26. Husson, S.J., Janssen, T., Baggerman, G., Bogert, B., Kahn-Kirby, A.H., Ashrafi, K., and Schoofs, L. (2007). Impaired processing of FLP and NLP peptides in carboxypeptidase E (EGL-21)-deficient Caenorhabditis elegans as analyzed by mass spectrometry. J. Neurochem. *102*, 246–260.
27. Husson, S.J., and Schoofs, L. (2007). Altered neuropeptide profile of Caenorhabditis elegans lacking the chaperone protein 7B2 as analyzed by mass spectrometry. FEBS Lett. *581*, 4288–4292.
28. Anderson, J.L., Reynolds, R.M., Morran, L.T., Tolman-Thompson, J., and Phillips, P.C. (2011). Experimental evolution reveals antagonistic pleiotropy in reproductive timing but not life span in Caenorhabditis elegans. J. Gerontol. A Biol. Sci. Med. Sci. *66*, 1300–1308.
29. Kaczmarczyk, A.N., and Kopp, A. (2011). Germline stem cell maintenance as a proximate mechanism of life-history trade-offs? Bioessays *33*, 5–12.
30. Petrulis, A. (2013). Chemosignals, hormones and mammalian reproduction. Horm. Behav. *63*, 723–741.

Current Biology

Supplemental Information

Olfaction Modulates Reproductive Plasticity through Neuroendocrine Signaling in *Caenorhabditis elegans*

Jessica N. Sowa, Ayse Sena Mutlu, Fan Xia, and Meng C. Wang

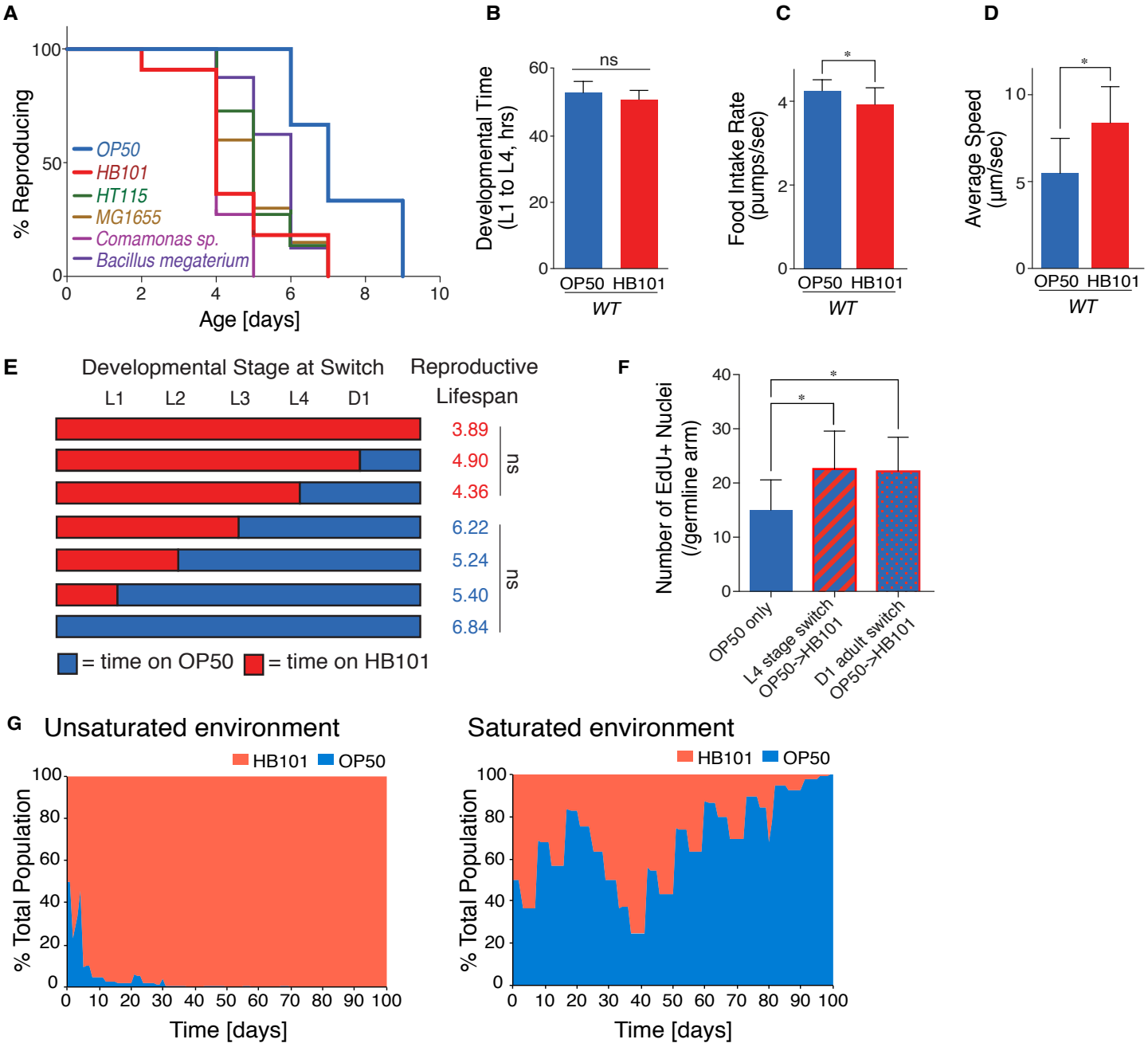

Figure S1: Related to Figure 1. (A) Variation of *C. elegans* reproductive lifespan on different bacterial diets. Reproductive lifespans of wild type (WT) *C. elegans* raised on various *E. coli* (OP50, HB101, HT115, and MG1655) strains and other bacterial species (*Bacillus megaterium* and *Comamonas sp*). (B) Average times are 53.1 ± 0.9 and 51.0 ± 0.9 hours for WT L1 larvae developing to the L4 stage when feeding on OP50 and HB101, respectively. ($p>0.05$, student's t-test) (C) Food intake rate of 1-day-old adult WT worms on OP50 (4.25 ± 0.08 pumps/s) vs. HB101 (3.92 ± 0.13 pumps/s). (*$p<0.05$, student's t-test) (D) Average speed of 1-day-old adult WT worms on OP50 (5.48 ± 0.82µm/s) vs. HB101 (8.37 ± 0.86µm/s). (*$p<0.05$, student's t-test). (E) Effects of diet switching from HB101 to OP50 on reproductive lifespan. WT worms feeding on HB101 were switched to OP50 at the L1, L2, L3, L4, or day 1 (D1) adult stage, and assessed for their reproductive lifespans. Worms switched during L1, L2, and L3 show reproductive lifespans similar to those of worms continuously raised on OP50 ($p>0.05$, log-rank test), whereas worms switched during L4 or D1 adulthood are more similar to those of worms continuously raised on HB101 ($p>0.05$, log-rank test). (F) Germline proliferation assessment by EdU incorporation of WT worms raised on OP50 and switched to HB101 at L4 or D1 adult stage shows that late exposure to HB101 is sufficient to cause a significant increase in germline proliferation rate. (*$p<0.05$, student's t-test). Data represented as mean ± SD. (G) Computational competition simulation of HB101 and OP50-associated reproductive strategies under different environments**.** In an unsaturated environment where population size is much smaller than environmental capacity (0.1%), animals with the HB101-like reproductive strategy will take over the whole population. In a saturated environment where population size is slightly over environmental capacity (102%), animals with the OP50-like reproductive strategy will take over the whole population. Results are from computational simulation as described in Supplemental Experimental Procedures.

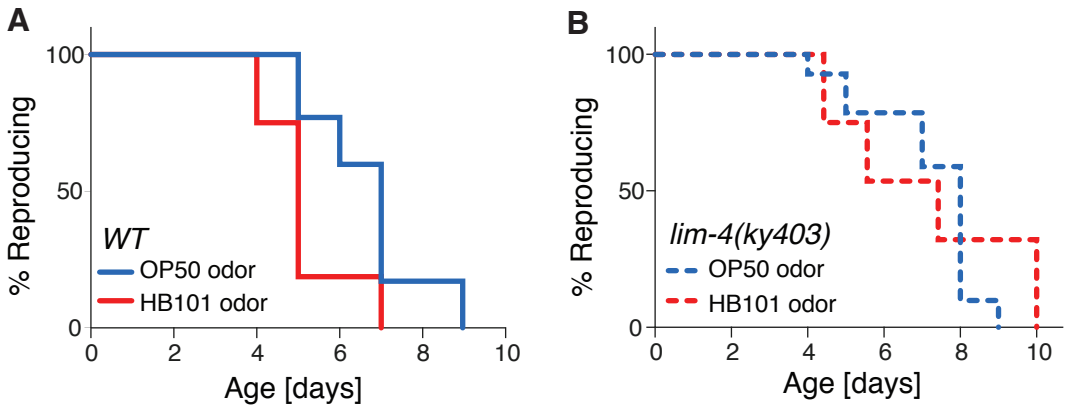

Figure S2: Related to Figure 2. HB101 odor fails to shorten reproductive lifespan in the *lim-4(ky403)* mutant. (A) Exposure to HB101 odorants shorten reproductive lifespan of WT worms feeding on OP50 ($p<0.05$, log-rank test). (B) Exposure to HB101 odorants does not shorten reproductive lifespan in the *lim-4(ky403)* mutant worms ($p>0.05$, log-rank test).

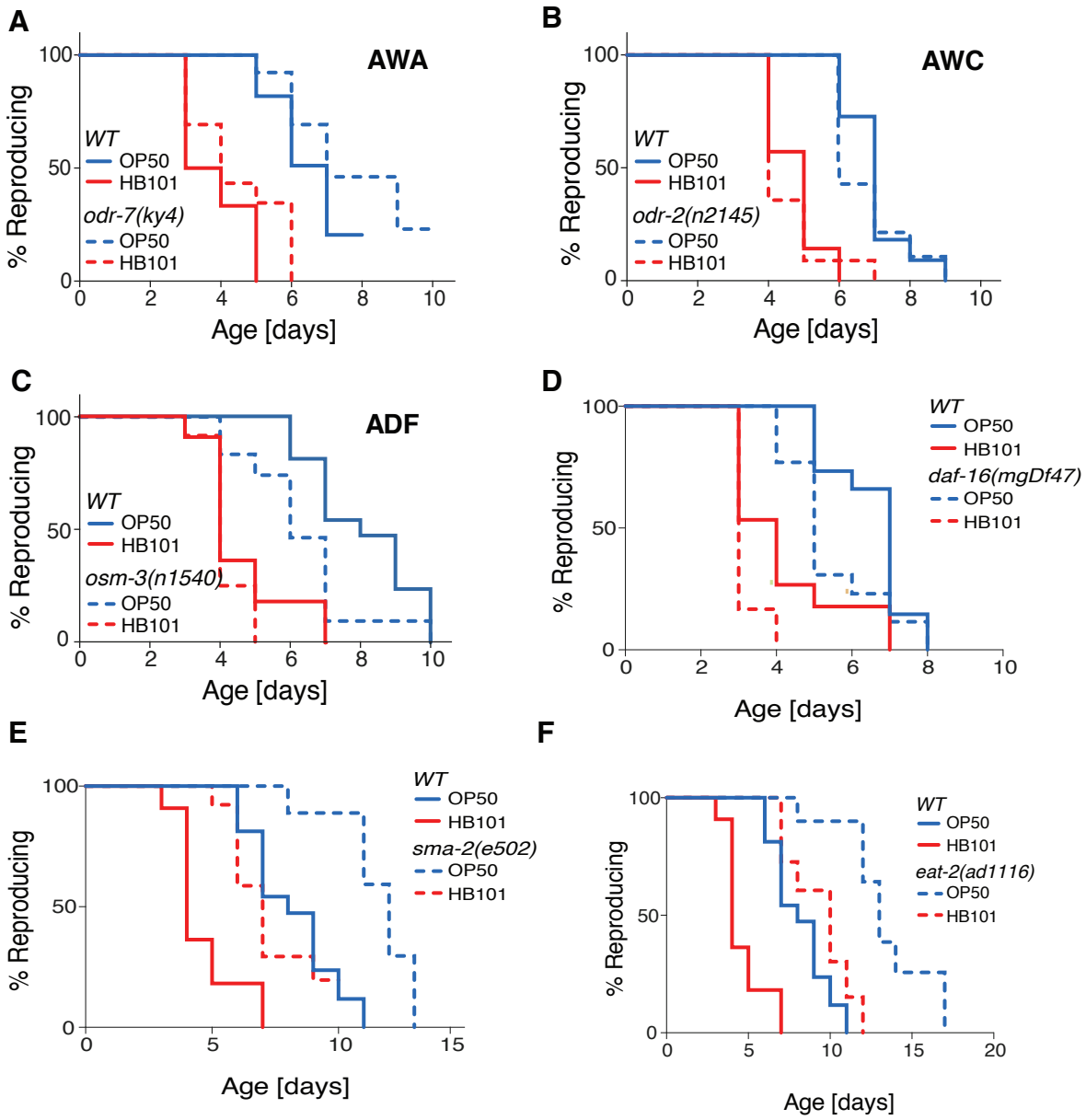

G

Mutant	Pathway	HB101	OP50	Extension	p value
N2	Wild Type	4.16	6.47	55.5%	<0.001
daf-16 (mgDf47)	FOXO/ Insulin/IGF-1 Signaling	3.17	5.42	70.1%	<0.001
sma-2 (e502)	TGF-β pathway	7.49	11.56	54.3%	0.006
eat-2 (ad1116)	Caloric Restriction	10.32	13.40	29.8%	0.014

Figure S3: Related to Figure 3. Genetic interaction analysis of HB101-mediated reproductive lifespan shortening and olfactory neuron function (A-C) or previously characterized pathways regulating *C. elegans* reproductive aging (D-G). (A) Reproductive lifespan of *odr-7(ky4)* AWA-defective mutants on OP50 vs. HB101 are significantly different ($p<0.01$, log-rank test). (B) Reproductive lifespan of *odr-2(n2145)* AWC-defective mutants show significant differences on OP50 vs. HB101 ($p<0.001$, log-rank test). (C) Reproductive lifespan of *osm-3(n1540)* mutants affecting ADF neurons show significant differences on OP50 vs. HB101 ($p<0.001$, log-rank test). (D) *daf-16(mgDf47)* mutants show a significant difference in reproductive span on OP50 vs. HB101. (E) *sma-2(e502)* mutants show a significant difference in reproductive span on OP50 vs. HB101. (F) *eat-2(ad1116)* mutants show a significant difference in reproductive span on OP50 vs. HB101. (G) Summary of genetic interactions with previously characterized regulators of reproductive aging.

Table S2. Summary of Reproductive Lifespan Analysis upon Diet Switching and Mixing

C. elegans Genotype	Bacterial Condition	Mean RLS ± s.d.	N	Censors	p value 1	p value 2
N2	OP50	6.844 ± 0.637	15	8	n/a	0.001
N2	HB101	3.889 ± 0.297	15	4	0.001	n/a
N2	OP50 -> HB101 @L1	3.933 ± 0.290	15	3	0.001	0.932
N2	OP50 -> HB101 @L2	4.444 ± 0.326	15	2	0.002	0.210
N2	OP50 -> HB101 @L3	4.018 ± 0.177	15	2	<0.001	0.452
N2	OP50 -> HB101 @L4	4.048 ± 0.238	14	2	<0.001	0.728
N2	OP50 -> HB101 @AD1	5.012 ± 0.423	14	2	0.028	0.062
N2	HB101 -> OP50 @L1	5.400 ± 0.378	15	3	0.086	0.015
N2	HB101 -> OP50 @L2	5.244 ± 0.447	15	1	0.041	0.054
N2	HB101 -> OP50 @L3	6.224 ± 0.605	14	3	0.506	0.012
N2	HB101 -> OP50 @L4	4.357 ± 0.202	14	0	0.003	0.586
N2	HB101 -> OP50 @AD1	4.899 ± 0.126	13	1	0.001	0.236
N2	OP50	8.184 ± 0.451	22	9	n/a	<0.001
N2	HB101	5.154 ± 0.220	26	3	<0.001	n/a
N2	1:1 HB101:OP50	5.000 ± 0.379	15	3	<0.001	0.504
N2	OP50	8.381 ± 0.649	12	3	n/a	<0.001
N2	HB101	4.286 ± 0.356	14	1	<0.001	n/a
N2	1:10 HB101:OP50	4.774 ± 0.341	15	0	<0.001	0.911
N2	1:100 HB101:OP50	5.353 ± 0.310	14	1	<0.001	0.377

Note:
AD1: day-1 adulthood
p value by Log-rank test, p value 1 comparison to OP50 within the group, p value 2 comparison to HB101 within the group.

Supplemental Experimental Procedures:

Strains

C. elegans strains used in this study: *N2* wild type, *odr-3(n2046), lim-4(ky403), odr-7(ky4), osm-3(n1540), odr-2(n2145), egl-3(gk238), egl-21(n476), sbt-1(ok901), sid-1(pk3321), sma-2(e502), daf-16(mgDf47),* and *eat-2(ad1116).* All strains used in this study were obtained from the Caenorhabditis Genetics Center**,** which is funded by NIH Office of Research Infrastructure Programs (P40 OD010440). *E. coli* strains: OP50, HB101, MG1655, and HT115. Other bacterial strains: *Comamonas sp., Bacillus megaterium.*

Transgenic strains

Is[AWB::ChR2] (raxIs15[str-1p::ChR2::sl2gfp])

Sequence 4kb upstream of *str-1* was PCR amplified from *N2* genomic DNA and inserted into polycistronic GFP vector with the pPD95_75 backbone (pMW11) using standard cloning techniques. Channelrhodopsin2 (ChR2) was PCR amplified from the plasmid pBA169_ChR2(H134R) (a gift from C. Herman) and cloned into the pMW11 vector using standard restriction site cloning. The plasmid pMW12_str-1p::ChR2::sl2gfp was injected into the germline of *N2* to make transgenic lines. *raxIs15[str-1p::ChR2::sl2gfp]* was integrated via gamma irradiation (4000 rads) and backcrossed to *N2* five times prior to reproductive lifespan testing.

Ex[AWB::unc-31^{KD}] (raxEx127[str-1p::unc-31sense;str-1p::unc-31antisense]) &

Is[AWB::unc-31^{KD}] (raxIs38[str-1p::unc-31sense;str-1p::unc-31antisense])

The *str-1* promoter was cloned into pJM23 plasmid backbone containing gateway attL recombination sites and sl2gfp sequence using standard cloning techniques (pMW13_str-1p::sl2gfp). *unc-31(exon 10-13)* sequence was PCR amplified from the plasmid pBS77_pgcy-13::unc-31(10-13)::sl2YFP (a gift from S. Xu) and recombined into pMW13_str-1p::sl2gfp vector in both sense and antisense orientations using Gateway LR recombination. The *str-1* promoter together with unc-31(10-13) (both sense and antisense) were PCR amplified from pMW14_str-1p::unc-31(10-13) sense::sl2gfp and pMW15_str-1p::unc-31(10-13) antisense::sl2gfp plasmids. Equal amounts of str-1p::unc-31(10-13) sense and str-1p::unc-31(10-13) antisense PCR products were injected into the germline of *N2* animals together with co-injection marker pmyo-2::mCherry. *raxEx127[str-1p::unc-31sense;str-1p::unc-31antisense]* array was crossed into *sid-1(pk3321)* background prior to experimentation. *raxEx127[str-1p::unc-31sense;str-1p::unc-31antisense]* was integrated via gamma irradiation (4000 rads) to create *raxIs38[str-1p::unc-31sense;str-1p::unc-31antisense],* which was backcrossed to *N2* five times before crossing back into *sid-1(pk3321)* background prior to experimentation.

Ex[AWB::TeTx] (raxEx126[str-1p::TeTx::sl2gfp])

Tetanus toxin light chain (TeTxLC) was PCR amplified from plasmid pGEMTEZ-TeTxLC (Addgene) using primers containing Gateway attL recombination sequences. TeTxLC sequences were then recombined into the pMW13_str-1p::sl2GFP vector using Gateway LR recombination. pMW16_str-1p::TeTx::sl2gfp plasmid was injected into the

germline of N2 animals together with co-injection marker pmyo-2::mCherry. *raxEx126[str-1p::TeTx::sl2gfp]* lines were used for experimentation.

Ex[AWB::odr-3] (raxEx125[str-1p::odr-3::sl2gfp])

Complete coding sequence of *odr-3* was PCR amplified from *N2* cDNA using primers containing Gateway attL recombination sequences. *odr-3* CDS was then recombined into the pMW13_str-1p::sl2gfp vector using Gateway LR recombination. pMW17_str-1p::odr-3::sl2gfp plasmid was injected into the germline of *odr-3(n2046)* animals together with co-injection marker pmyo-2::mCherry. *odr-3(n2046); raxEx125[str-1p::odr-3::sl2gfp]* lines were used for experimentation.

Reproductive lifespan assay

Worms were grown for at least 2 generations well fed on standard NGM plates seeded with OP50 prior to reproductive lifespan assays. Synchronized L1 larvae were plated on 3cm NGM plates without antibiotic seeded with either OP50 or HB101 *E. coli.* 15-20 worms were picked individually to 3cm plates at L4 stage, and moved to a fresh plate each day until 3 consecutive days without progeny production. Worms were kept at 20°C for the duration of reproductive lifespan testing. After transferring, plates were stored at RT and checked for progeny after 2 days. For each individual, the last day of live progeny production was determined as the day of reproductive cessation. Animals that could not be followed until reproductive cessation due to death, internal hatching, or crawling into agar were considered as censors on the last day on which they were known to reproduce. If day of censor could not be definitively determined, animals were

removed from analysis. Statistical analyses were performed using the Kaplan-Meier survival method followed by a log-rank test (SPSS software, http://www-01.ibm.com/software/analytics/spss/).

Late life fertility

Worms were grown for at least 2 generations well fed on standard NGM plates seeded with OP50 prior to assay. Synchronized L1 larvae were plated on NGM plates without antibiotics seeded with either OP50 or HB101 *E. coli.* Upon reaching adulthood, hermaphrodites were transferred to fresh plates every 2 days until late adulthood. At the indicated day of adulthood, individual aged hermaphrodites were transferred to 3cm plates with 2 day-2-old young *N2* males. Hermaphrodites were mated for 48hrs, after which males were removed. Plates were checked for progeny production after 3 days. 10-15 hermaphrodites were used for each experiment and each experiment was repeated at least 2 times independently. The number of hermaphrodites in each group that were able to resume reproduction after mating was compared using a Fisher's exact test.

Food choice assay

Synchronized L1 larvae were plated on standard NGM plates seeded with OP50. At the first day of adulthood, worms were washed off plates with M9 buffer and washed four more times with M9, then concentrated into 90μL M9. OP50 and HB101 *E. coli* were cultured overnight in LB, and bacterial concentrations were normalized between OP50 and HB101 based on bacterial counts. 100mm square NGM plates were seeded with 200μL of 3X concentrated OP50 and HB101 culture in opposite corners, 40mm apart.

Plates were dried in sterile hood, and 2μL of 10% Na-azide was added to each *E. coli* lawn. Food choice plates were prepared freshly before adding worms. 30μL of washed and concentrated worms (~100 worms) were added to the center of each food choice plate. Worms were allowed to choose for 4hrs until all worms were paralyzed. Each food choice experiment was performed in technical triplicate, and repeated 3 times independently.

EdU incorporation

Thymidine-deficient *E. coli* strain MG1693 was grown in media containing 100mM EdU for 24hrs, then seeded on NGM plates. Synchronized 1-day-old adult worms were washed several times with M9 buffer to remove residual bacteria, then placed on EdU-labeled MG1693 plates and allowed to feed for 1hr. The germline was dissected out as previously described [S1] and stained using Click-iT® EdU Alexa Fluor® 647 Imaging Kit (Invitrogen). Coverslips were mounted using Vectashield® mounting medium with DAPI, and Z-stack images of each germline captured using an Olympus FluoView1000 laser scanning confocal microscope at 40X magnification. Image analysis was performed using ImageJ software (from NIH, http://imagej.nih.gov/ij/download.html). Analysis based on the number of EdU^+ nuclei counted in middle slice of z-stack for each germline. 15-30 germlines were analyzed for each group, drawing from 3 independent EdU feeding experiments. Numbers of EdU^+ nuclei were compared between diet groups using student's t-test with Bonferroni correction.

Optogenetics

Is[AWB::ChR2] transgenic and *N2* control worms were raised in the dark on NGM plates seeded with *E. coli* containing 500μM all-trans-retinal [S2]. Beginning at L4 stage, worms were exposed to 470nm blue light from LEDs (intensity 10μW/mm^2) for 1hr per day for duration of experiment. After blue light exposure, worms were transferred to fresh plates daily in the dark room and reproductive lifespan assessment was performed as previously described.

Progeny production analysis:

10 synchronized L4 hermaphrodite larvae were transferred to fresh plates every day and the number of progeny was counted daily until reproductive cessation. The total number of progeny per hermaphrodite was calculated. Hermaphrodites that censored prior to reproductive cessation were excluded from analysis. The experiments were performed twice at 20°C. HB101 and OP50 groups were compared using a student's t-test.

Developmental time measurement:

10 synchronized L1 larvae were allowed to develop at 20°C. The animals were examined every half hour to note the transition to L4. If any, the L4 larvae were removed from the population. The time from L1 to L4 when the animal was removed was recorded for each individual. HB101 and OP50 groups were compared using a student's t-test.

Locomotion activity measurement:

Age-synchronized day 1 adult worms on either HB101 or OP50 worm plates were recorded for their spontaneous movement for one minute using an SMZ1500 stereo

microscope (Nikon) connected to a C11440 camera (Hamamatsu). Individual worms were tracked using NIS Elements AR imaging software (Nikon) and average velocity (μm/sec) was calculated. HB101 and OP50 groups were compared using a student's t-test.

Pharyngeal pumping measurement:

1-day-old adult worms on either HB101 or OP50 were recorded for 1 minute using an SMZ1500 stereo microscope (Nikon) connected to a C11440 camera (Hamamatsu). The number of pharyngeal contractions in each second interval was calculated. For both groups, the mean of 10 animals was compared using a student's t-test.

Computational simulation of population growth competition

To model the growth dynamics of organisms that utilize either HB101 or OP50 associated reproductive strategies, we used the following equations and parameters:

1. The developmental time from eggs to adults is 3 days; and the numbers of daily progeny production over 10 days for HB101 and OP50 are:

$$HB101: r = \{100, 175, 25, 0, 0, 0, 0, 0, 0, 0\}$$

$$OP50: r = \{30, 100, 100, 30, 15, 10, 7, 5, 2, 1\}$$

2. The population growth is logistic

$$\frac{dN}{dt} = N \cdot s$$

$$s = \frac{K - N}{K} \ , s = 0 \ if \ K > N$$

K represents environmental capacity for reproduction, and N represents the number of effective populations including reproducing adults (a_i) and non-dauer larvae (l_j):

$$N_d = \sum_{i=1}^{10} a_{i,d} + \sum_{j=1}^{3} l_{j,d}$$

3. The number of day-1 adults (a_1) is the number of day-3 larvae (l_3) that can survive to adults in the next day;

$$a_{1,d+1} = l_{3,d} \cdot (0.6 \cdot s + 0.4)$$

while for day-2 to day-10 adults (a_{i+1}), their numbers are determined by the number of adults that can survive to the next day.

$$a_{i+1,d+1} = a_{i,d} \cdot (0.6 \cdot s + 0.4)$$

4. Progeny production by adults that have resource to reproduce determines the number of day-1 larvae (l_1).

$$l_{1,d+1} = \sum_{i=1}^{10} (a_{i,d} \cdot r_i \cdot s)$$

5. When the environment is harsh ($if\ s \leq 0.1$), half of day-1 larvae will form dauers (D) and half of them will become day-2 larvae (l_2).

$$D_{d+1} = D_d + l_{1,d} \cdot (0.6 \cdot s + 0.4) \cdot 0.5$$

$$l_{2,d+1} = l_{1,d} \cdot (0.6 \cdot s + 0.4) \cdot 0.5$$

The number of day-3 larvae (l_3) will be the sum between day-2 larvae and arrested day-3 larvae that can survive to the next day.

$$l_{3,d+1} = l_{2,d} \cdot (0.6 \cdot s + 0.4) + l_{3,d} \cdot (1 - 0.6 \cdot s - 0.4) \cdot s$$

6. When the environment becomes better ($if\ s > 0.1$), no dauers are formed and day-2 larvae are developed from day-1 larvae.

$$D_{d+1} = 0$$

$$l_{2,d+1} = l_{1,d} \cdot (0.6 \cdot s + 0.4)$$

At the same time, some dauers will become day-3 larvae. Therefore, the number of day-3 larvae is

$$l_{3,d+1} = \left(l_{2,d} + D_d\right) \cdot (0.6 \cdot s + 0.4) + l_{3,d} \cdot (1 - 0.6 \cdot s - 0.4) \cdot s$$

Based on the above equations, we have performed computational simulation of growth competition between two populations using HB101 and OP50 reproductive strategies over 100 days ($d = 100$). In the simulation, K is set to 20,000, $l_{1,1}$ is set to 0, and $a_{1,1}$ for HB101 or OP50 is set to increase from 20 to 20,480 (2-fold in each increment). The initial N_1 is increased from 40 to 40,960. When $N_1 < 20480$, the population with HB101 reproductive strategy will prevail the competition; when $N_1 \geq 20480$, the population with OP50 reproductive strategy will prevail the competition. In Figure S4, the results from $N_1 = 40$ and $N_1 = 20{,}480$ are presented as examples.

Supplemental References:

S1. Crittenden, S.L., and Kimble, J. (2008). Analysis of the C. elegans germline stem cell region. Methods Mol Biol *450*, 27-44.

S2. Schultheis, C., Liewald, J.F., Bamberg, E., Nagel, G., and Gottschalk, A. (2011). Optogenetic long-term manipulation of behavior and animal development. PLoS One *6*, e18766.